

Science and art belong to the whole world,
and the barriers of nationality vanish before them.

Goethe, 1813

The relative velocity of the winds may be best ascertained
by finding the relative velocity of the clouds.

Dalton, 1793

Chapter 2

Observing the Atmosphere

Purpose: To evaluate the different sources of data used in this book to describe the atmosphere. Some differences between observing systems and reanalysis data are highlighted. Some implications of the primary balances are discussed. The motivation for, and some consequences of averaging are described.

2.1 Observational data

2.1.1 Overview

Meteorological observations are essential for understanding the atmosphere. A great many observations are routinely taken each day in every country and across every sea. These data are freely shared among the countries of the world through the World Meteorological Organization (WMO). Atmospheric science requires data sharing because the atmosphere recognizes no national boundaries.

Data studied in this book have been heavily processed. The data are collected and checked for errors. The data are then transferred by some means onto a regular grid. Nearby observations for various devices often disagree. The observations are assigned relative weights based upon the observing devices' reliability and other considerations. Additional processing may occur to bring the various fields into a specified mathematical balance. Strictly speaking, data that have undergone such processing are called 'analyses' and not 'observations'. For convenience analyses in this book will be labeled as "observed" data. Creating analyses often involves processing the data with a computational model of the global atmosphere.

Observing the atmosphere with sufficient detail is a great undertaking. The difficulty and expense of the task have spawned creative solutions to the problem of acquiring accurate data. For example, in Dalton's time, upper air information was obtained largely by watching the clouds: their speed could be determined by tracking the motion of their shadows from a hilltop. Two hundred years later, high technology satellites gather wind data using the same basic idea.

A primary task of this chapter is to peek at the sources of data that contribute to many of the plots to come. Analyses of observations were interpolated onto regular grids for plotting the figures in this book. Observing the atmosphere is an enormous task. Though a heroic effort is made to sample the atmosphere, the available observational network has biases. Another huge effort merges diverse observations to form coherent global datasets as needed to study the general circulation. A major advance since the first edition of this book (Grotjahn, 1993) has been the creation of 'reanalysis' datasets. These popular reanalyses improve upon earlier global datasets in several ways, such as: by including more types of data and by using a consistent global model for the duration of each reanalysis. The documentation for each reanalysis (e.g. Kalnay et al., 1996; Kanamitsu et al., 2002; Uppala et al., 2005) always discusses the sources and limitations in the data. For example, the first NCEP reanalysis dataset (Kalnay et al., 1996) assigned a category to each variable to indicate how strongly the **reanalysis values were influenced by observations versus model calculations**. Some variables (like temperature and horizontal wind) are strongly influenced by observations. Other variables, like humidity and surface temperature are influenced by observations and model. Some other variables (like vertical motion and surface fluxes) are model products that are not directly observed. To validate the observations shown, their consistency with other observations and with theory is stressed throughout this book.

Time is an ally in this task. Meteorologists emphasize the length of data record to improve the capture of the atmospheric variability as well as to estimate better the time mean. The length of time to obtain an adequate representation is somewhat subjective and varies with the variable considered. Once the data have been gathered, checked, and somehow interpolated onto a grid, there remains one more problem to consider. The "four-dimensional" space and time-varying atmosphere has exceedingly complex structure and evolution. Averaging over time (and over one or more space dimensions) makes the huge quantity of information manageable to the mind. Beyond fitting the data onto a two-dimensional page, averaging is usually directed to reveal useful concepts or dynamical relationships. However, all **averaging is a filter**, and knowing what the filter removes is important as well.

The discussion above leads to an emphasis here upon higher quality and longer period data. The preferred data are so-called 'reanalysis' datasets from NCEP (here called: NDRA2; Kanamitsu, et al., 2002) and from ECMWF (here called ERA-40; Uppala et al., 2005). These

reanalysis datasets are so-named because historical weather data have been reanalyzed with a recent atmospheric model to apply a consistent processing of the observations available. While these two datasets are a huge advancement in analyzing the atmosphere, the two are not always in agreement and those differences will be noted in later chapters. Grotjahn (2008) has a comprehensive global comparison of the NDRA2 and ERA-40 data for numerous variables. Where available, longer time averages are shown. However, a major **upgrade of the observing system occurred in 1979** as part of the Global Weather Experiment. The upgrade notably expanded satellite-based observations and provided more coverage of the Earth, especially in regions where the observing stations have gaps. Over the next decade additional satellite-based observations were deployed. These additional observations create notable differences in measured properties of the atmosphere before and after 1978 (e.g. Kistler, et al., 2001, p. 252; Trenberth and Smith, 2005, 2006) hence data after 1978 are generally selected in this book.

2.1.2 What data are needed?

Certain **variables are essential for understanding the general circulation**. Pressure, radiation (solar and terrestrial), temperature, water vapor and wind speed and direction are needed at levels from the Earth's surface upwards into the high stratosphere. At the surface, these quantities along with precipitation and the surface energy budget components are required. Surface energy budget includes radiation along with sensible and latent heat fluxes. In addition, the radiative properties at the top of the atmosphere (TOA) are needed. Some scientists (GCOS Steering Committee, 2010) argue that some key variable gases present in the atmosphere (CO₂, O₃, CH₄, and aerosols) need be discussed, though those are more important for climate change than for the overview of the general circulation presented here. Some oceanic variables are important for understanding the atmosphere's general circulation, primarily: sea surface temperature (SST), heat transport by currents, and surface energy balance.

2.1.3 Some implications of different balances

In chapter 1 and Appendix C, some primary balances are discussed for the atmosphere. In this section some observational data needed to study the primary balances are described.

The circulation is in hydrostatic balance, (C.12) except at very high altitudes or on small scales of motion (such as inside a cumulus cloud). Hence, for the large scale circulations described here it is reasonable to assume hydrostatic balance. What are the implications of strongly hydrostatic balance? Approximate **hydrostatic balance has three implications** for compositing observations. First, the balance arises from neglecting vertical accelerations, hence

vertical motions tend to be small and the primary motion is horizontal. Second, hydrostatic balance expresses pressure in terms of the density field *or* in terms of the (virtual) temperature distribution. Therefore, only density *or* temperature need be measured. Indeed, many measurements are taken using pressure as the independent variable for this reason. Hydrostatic balance also means one does not need to measure density as well as pressure since one can express density, ρ in terms of pressure p . Third, since the motion is nearly horizontal, many atmospheric properties can be fruitfully examined in two-dimensional, horizontal slices. Though one should not restrict oneself to this “two-dimensional” view, this viewpoint simplifies the visualization of motion and other properties.

The geostrophic approximation (C.36) and (C.37) is much less predominant than the hydrostatic, but it is a **useful tool for qualitative interpretation**. Geostrophic balance holds reasonably well for air that is: outside the tropics, outside the boundary layer, and moving with a large scale circulation. What are the **implications of geostrophic balance**? First, the geostrophic assumption will delete circulations that have vertical motions. Non-geostrophic motions of any type (that is ageostrophic motions) are quite important in maintaining many features. Indeed, the **Hadley and Ferrel cells *must* be at least partly ageostrophic** since they include nonzero vertical velocity. Second, geostrophic balance strongly ties the horizontal winds to horizontal pressure gradients. Geostrophic balance thus provides a **link between features seen in the mass and horizontal wind fields**. In early attempts at deducing the global structure of the atmosphere, this balance was sometimes incorporated to deduce winds from geopotential heights, and *vice versa*.

When hydrostatic balance and the ideal gas law, (C.1) are combined, one obtains the hypsometric equation (C.13). The hypsometric relation indicates that the vertical spacing between two pressure levels is proportional to the average virtual temperature between those levels. What is the **implication of that balance**? Warmer temperatures will be linked with deeper spacing of pressure (or correspondingly, geopotential height) fields and *vice versa* for colder temperatures. This provides a basic consistency check for the data shown here as well as a powerful means to **link features seen in the thermal and mass fields**.

A similar linkage between fields flows from thermal wind (shear) relations, such as (C.38)-(C.40). A horizontal temperature gradient implies a horizontal pressure gradient (from the hypsometric relation). In turn, **temperature gradient implies a wind shear** (from geostrophic balance). Since surface winds are generally light, stronger upper level winds lie above stronger horizontal temperature gradients.

2.2 Observational technologies

2.2.1 Fixed-location observational network

The **fixed-location network** refers to observations that are made from the same location on Earth at frequent intervals. The two main components of this network are ~1000 *upper-air* stations and ~9,500 stations that only make surface observations. Personnel at upper air stations release radiosondes or pilot balloons (pibals) to measure data above the ground. Pibals estimate wind from the rising balloon's horizontal drift. Radiosondes measure temperature, pressure, humidity, wind speed, and wind direction at regular intervals including at the *standard pressure levels*. (The standard levels are: 1000, 850, 700, 500, 400, 300, 250, 200, 150, 100, 50, and 10 hPa.) Depending upon the local conditions, additional observations may be reported at *significant* levels. Significant levels are identified where one or more of the measured variables differ from a linear vertical trend by more than a specified amount. The principal **advantages of station-based data** are: 1.) high accuracy due to direct measurement instead of remote inference and 2.) consistency. By consistently measuring from the same geographic locations over time, subtle changes in climate over time may be detected. **Table 2.1** summarizes the accuracy and distribution of the station-based and other significant observing systems discussed in this chapter.

Station-based observational data have several drawbacks. The main problems are as follows. 1.) The spacing between stations is irregular. 2.) There is a noticeable bias for land areas, with poor coverage over the oceans. 3.) There is a bias toward clear skies and light winds, especially for upper atmospheric data (e.g. van Loon, 1972, p.87). 4.) The data taken along the track of a balloon may not be representative of the surrounding environment. Nappo et al. (1982) discuss this last point. Bruce et al. (1977) also examined representativeness by comparing simultaneous rawinsonde reports at adjacent stations. A clear sky bias results from visual tracking methods. Once a pilot balloon enters a cloud, it cannot be tracked. When a radiosonde is released near the jet stream, it may be blown over the horizon before it can complete its rise through the atmosphere. This bias toward light winds is one reason why comparatively few radiosondes report information above the lower stratosphere (another reason concerns solar heating of the sonde thermistor). Even when kept in sight, a 200km drift over a 90 minute ascent (McGrath, 2006) introduces a notable location error if plotted at the station location. There can be errors in the measurements and in the data transmission to the central receiving site. Quality control measures reduce these errors substantially in reanalysis data (Kistler et al., 2001).

The distribution of radiosonde observation stations is shown in **Figure 2.1**. The figure gives a sense of the amount of data each station provides, with darker and larger dots indicating a more complete daily record. The network at different times is shown here since this book relies upon data averages beginning in 1979 and the observing system properties (coverage, frequency, etc.) have varied over that time. The **station coverage is generally excellent over the land** areas in

middle latitudes. In general, the tropics are sampled poorly, including many land areas. The oceans are sampled very poorly by this network. The lack of station coverage is quite serious in the Southern Hemisphere. The coverage over North America and Europe and southern Asia is similar in both periods while coverage over Australia has improved. Parts of South America have better coverage but other parts have less in 2001 compared with 1979. Coverage declined over Africa and much of the former Soviet Union. As for the frequency of coverage, during May 1984; 855 (of 1,024 registered) radiosonde stations and 373 pibal stations were active. Nearly a decade later, 820 radiosonde stations (600 pibal) provided data from 1,200 (1,000) ascents each day (WMO, 1991). In general, only about 75% (Mohr, 1984) of these stations send in data at any one observing time. The ERA-40 dataset used 2274 (606) ascents of radiosondes (pibals) per day during 1979-1990 and 1456 (676) per day during 1991-2001. The first NCEP reanalysis (Kistler et al., 2001) used 36,000 to 44,000 radiosonde ascents per month from 1979-1997. The figure may be compared with figure 2.1 in Grotjahn (1993). Grotjahn (1993) showed active radiosonde and pibal stations during May 1984 to have similar locations with one major exception: most of the upper air stations in equatorial Africa were pibal stations. Accordingly, the winds are better sampled over West Africa than are other variables.

The fixed-location **surface observation network has many more stations** (Figure 2.2) than upper air stations. While many of the same drawbacks apply as for upper air stations, the sampling in tropical regions is better. The coverage differs for different variables and only stations providing monthly mean data considered to be of high quality are shown in Figure 2.2. The ERA-40 data incorporated about 34,000 (37,000) surface *observations* per day, including data from ships, in the 1979-1990 (1991-2001) time period. In recent decades there are many moored buoys which are technically fixed-location, but these platforms are discussed below along with drifting buoys.

2.2.2 Satellite-based observations

To obtain reasonable global coverage, other sources of data fill the gaps between the radiosonde stations. A primary tool for filling those gaps is to mount sensors on geostationary and polar orbiting satellites. (WMO, 2008, provides an overview of satellite observation systems.) Figure 2.3a shows the typical **temperature sounding coverage from an operational polar orbiting satellite**. Swaths are shown and the times of passage overhead of the spacecraft are indicated. Within each swath are circles where each circle represents a vertical profile of temperatures retrieved by the TIROS-N satellite using the MSU device. A MSU device has been used on several satellites since 1979. During more recent years, other sounding devices have been developed for satellites, such as the AMSU-A. These later devices sample other frequencies of

the electromagnetic spectrum and generally interrogate smaller “spots” over different swaths beneath the polar orbiting satellite. **Figure 2.3b** illustrates the numbers of soundings from the MSU that are incorporated in the latter half of the ERA-40 data. About 6,000 temperature soundings were made each day by TIROS-N early in the period of interest (Halem et al., 1981). By the early 1990’s, about 10,000 soundings were recorded per day (WMO, 1991). More recently, the geostationary satellites have been fitted with sounding devices as well. On average, the ERA-40 dataset incorporated about 131,000 (181,000) satellite radiance values each day during 1979-90 (1991-2001).

Satellite-mounted devices **estimate temperatures from measuring infrared emission** from segments of the atmospheric long wave emission spectrum. The radiation emitted by an object is related to the object temperature. Radiation is absorbed, emitted, scattered, and transmitted through the atmosphere. In general terms, the peak emission from an atmosphere will be near the level where the optical depth equals one. Less emission occurs from other atmospheric levels. The profile of optical depth varies with the wavenumber of the radiation and with the absorbing gas. Consequently, these relationships can be “inverted” to obtain estimates of temperature over broad atmospheric layers. A more detailed explanation of the method is beyond the scope of this text. The scheme used for the ERA-40 data is described in McNally et al. (2000); these data are an “analysis” meaning the soundings are generated as corrections to a first guess produced by a forecast model’s temperature sounding predicted for each “spot”. In addition to the imprecision in the inversion process, the data must be calibrated to accommodate spurious trends introduced by changes in the instrument sensitivity and orbit of the satellite. A more recent additional way in which satellites can generate temperature soundings is by using radio occultation of signals passing through the limb of the atmosphere between two GPS satellites (e.g. Ware et al., 1996) and generally high in the atmosphere where the moisture content is low.

The calculation of temperature from the radiance is difficult and imprecise. **Estimation of the temperature error** requires creating a common interface, for example, satellite data are essentially a weighted average over a range of levels, so to compare with radiosonde data (reported at specific levels) the radiosonde data must be averaged with similar weighting. Also, the satellite averages over a horizontal ‘spot’ while the radiosonde only senses along its ascent path. When that comparison is made, the satellite estimates differ by: ~0.3K for the lower atmosphere in the tropics to ~1K in high latitudes over time averages (Spencer and Christy, 1992). Gridded datasets derived from satellite data and radiosonde data have been compared (Hurrell, et al., 2000) and show root mean square (rms) differences ~0.6 K over the Northern Hemisphere continents (and larger rms values in the tropics). When the comparison is made the other way, assigning the satellite temperatures to specific levels, then typical rms differences between satellite and radiosonde values are 1.5-2.5°C (e.g. Smith et al., 1979). It should be noted

that temperatures measured by nearby radiosonde ascents can differ by a few degrees. Ware et al. (1996; their table 1) summarize temperature error standard deviations for several observing systems as a function of height, including radiosondes (1.3-2 K) and satellites (3.9-4.7K for clear skies; 4.6-5.6K for cloudy skies). The values within the parentheses are values for elevations in the troposphere. Clearly, the size of the error depends on whether single values at a point are used or whether averages over regions are taken. Ware et al. stress that these error estimates are generally higher than the absolute error of a particular instrument (e.g. 0.5K for some radiosondes) because they also include how well a point measurement represents a larger area (representativeness) and systematic (i.e. non-random) errors. Hence, radiosonde temperatures are generally quoted as 1-2K (Luers and Eskridge, 1995) and satellite temperature errors a bit larger. The data are likely adequate for the purposes here because large scale, time averaged (often zonally-averaged) depictions of the gross features of the general circulation are emphasized here and because the reanalysis data displayed were developed with considerable effort to reduce these types of errors.

Wind information can be obtained from satellites as well. Such winds go by several names: cloud-track winds (CTW), cloud drift winds, cloud motion winds, atmospheric motion vectors, satellite winds, visible winds, sounder water vapor winds. The different names arise from different techniques and instruments. Upper atmospheric winds can be deduced by following the motions of cloud features between two or three sequential images taken 15 minutes to one hour apart by a geostationary satellite. The distance travelled by a feature divided by the time interval between the images gives the velocity. Different operational centers have automated the process to varying degrees by searching for distinct cloud features or strong gradients, both moved passively by the winds. Naturally, only one level of cloud is visible at any one point on the globe, as can be seen in Figure 2.4. Other winds can be obtained by tracking features in the water vapor infrared channel. The vector motion is assigned to an altitude by one of two means. One method is to assign all the winds to fixed altitudes. Though the features tracked undoubtedly varied greatly with height, the winds shown in Figure 2.4 were assigned to three fixed levels. The other method assigns the winds based on radiances of the tracked feature in certain infrared channels. By comparing the temperature deduced from the radiances with a nearby temperature profile from a radiosonde, satellite sounding, or grid point analysis, the level of the CTW can be assigned.

Even if the cloud feature's elevation is known, the air speed at that level could be different. The wind may blow around the cloud. Some evidence suggests that deep clouds tend to move with the vertical average velocity of the winds surrounding the cloud (Hasler et al., 1979).

Hasler et al. (1979) compared CTW with in situ measurements. Over a five year period, they flew an aircraft through 81 clouds for which satellite winds were obtained. Most of the

clouds were low-level cumulus. They studied five cirrus clouds. The researchers chose several locations in the tropics and subtropics of the north Atlantic and Caribbean. For low cumulus clouds, the difference between the wind speed at the cloud base and the CTW was only 0.9 m/s to 1.7 m/s. For the limited sample of cirrus clouds, the difference between the mean wind in the cloud layer and the CTW was 2.3 m/s. These estimates are considerably less than errors found by comparing CTW data with nearby radiosondes. Those latter error estimates range from about 5 m/s for low level winds to 10–14 m/s for high level winds (Halem et al., 1982). The large difference between error estimates made using in situ measurements versus *analyses* from radiosondes illustrates the problem of representativeness. Specifically, the CTW averages the wind speed over a larger horizontal and vertical area than does a radiosonde balloon.

Thirty years ago about 6,000 CTW were logged each day (Halem et al., 1981). A decade later, about 7,000 CTW were obtained each day from the five geostationary satellites (WMO, 1991). Many more satellite derived winds were obtained in more recent times. The ERA-40 data used about 6,600 and 46,000 satellite winds per day in the 1979-90 and 1991-2001 periods, respectively.

Satellites can also estimate surface winds over the ocean by measuring the scattering of microwaves emitted by a polar-orbiting satellite, reflected from capillary waves on the ocean surface, and received by the satellite. Such devices have been in regular use since mid-1991. Wind speed is estimated since the reflection is stronger for stronger winds (rougher ocean surface). Wind direction is estimated from how the backscatter varies with the angle of the satellite to the wind as the satellite moves along its orbit. Freilich and Dunbar (1999) compare NSCAT scatterometer winds with co-located buoys and estimate an rms error of 1.3m/s and directional errors less than 17 degrees. About three quarters of the ocean is covered each day (Pegion et al., 2000). ERA-40 used about 7500 scatterometer observations per day during 1991-2001.

Some weather satellites estimate the amount of **water vapor present in the middle troposphere** (600–300 hPa elevation). An electromagnetic spectral band (usually between 5.7 and 7.1 μm) is examined. Water vapor absorbs radiation in this band (between the visible and thermal infrared channels). Estimates of water vapor were first made using instruments on polar orbiting satellites in the early 1970s (e.g., Steranka et al., 1973). Later, this band has been available on geostationary satellites (e.g., Morel et al., 1978). The water vapor distribution also can be scanned for identifiable features that can be tracked between consecutive satellite images. Hence, winds in cloud-free areas can be estimated by tracking these features using the same techniques as for CTW. Stewart and Hayden (1985) estimate the error in these “water vapor winds” to be 4–7 m/s. Satellites can also estimate total column water vapor (in units of length this is the “precipitable water” depth if all the moisture in the column was converted to liquid water). The

TOVS radiances from different spectral bands, each emphasizing a different range of elevations, can be used to construct precipitable water amounts in more than one layer. These data are blended with other observations in global datasets (e.g. Randel, et al., 1996) including reanalysis datasets. Soden and Bretherton (1994) found some satellite estimates to differ from ECMWF analyses by 2-3 kg/m². Liu et al. (1992) find an rms difference with ECMWF analyses of about 4 kg/m².

Of course, weather satellite imagery shows the pattern of clouds and infrared imagery is also constructed to show information about cloud heights. Until recently, forecast models did not use cloud information directly. In the past few years a new emphasis has been placed upon measuring the clouds. A principal outgrowth was the establishment of the International Satellite Cloud Climatology Project (ISCCP) in 1983. The main goals of ISCCP (Schiffer and Rossow, 1985) include accurate measurement of radiative properties of the earth in addition to establishing an accurate cloud climatology. Cloud amount and type have a crucial effect upon the radiative balance of the earth.

2.2.3 Other observing systems

Other sources of observations include commercial aircraft, drifting buoys, merchant ships, research aircraft with dropsondes, and constant level balloons. [Table 2.1](#) summarizes these measurement systems and the characteristic errors for each.

Commercial aircraft can provide meteorological data by several means. One method is to collect in-flight and post-flight manual reports (labelled “AIREP”) at regular intervals (e.g. every 10 degrees longitude). AIREPS include cloud information (amount, cover, height), temperature, and wind. This system typically provides 4500 reports per day from 3000 aircraft. In the 1980s an alternative observing system was tested whereby some wide-body commercial aircraft were outfitted with Aircraft Meteorological Data Relay (AMDAR) systems (ASDAR units use a satellite link; ACARS use a radio link). Some details about the AMDAR program are shown in [Table 2.1](#) and are drawn from Sparkman and Smidt (1985) and Drüe et al. (2008). These commercial aircraft systems provide temperature and wind data at flight level (300–200 hPa). International flights over the oceans and over the tropics were particularly useful. A “sounding” is taken during the ascent and descent of takeoffs and landings. The total number of aircraft observations used by ERA-40 are ~4100 and ~26,000 in the 1979-90 and 1991-2001 time periods.

Many **merchant ships** take surface observations along the major ocean shipping lanes (especially the northern Atlantic and Pacific oceans). Seven thousand of these so-called “ships of opportunity” provide most of the same data as synoptic land stations in the 1980’s. More

recently, the number of such ship reports has declined substantially. A semi-automated system was developed whereby radiosondes are released from merchant ships. Initially tested in the North Pacific, the Automated Shipboard Aerological Program (ASAP) was expanded to the Atlantic Ocean. With generally one to two dozen ships reporting twice per day, ~6000 soundings are taken in a year. The device takes standard radiosonde measurements: wind speed and direction, temperature, humidity, and pressure. As with ASDAR, the data are automatically transmitted to satellites. The automation reduces the data transmission time from 12–18 hours to 1–1.5 hours and the error rates from an estimated 30% to 1%.

Buoys are very useful for providing surface pressure in remote ocean areas. Some buoys also provide air temperature and wind speed. The main role of buoys is to fill in major gaps in the surface observational network. Buoys are often placed where merchant ships are infrequent (such as the southern oceans) or where there is a critical need for closely-spaced observations (such as in the Great Lakes). Some buoys are tethered, but most oceanic buoys are set adrift. Ships or aircraft can deploy some buoys. Aircraft deployment allows gaps in the drifting buoy network to be filled more easily than before. The buoys report directly to a polar orbiting satellite. Most buoys are operational for several months. The number of buoys operational at a given moment has grown over time with ~300 (WMO, 1991) in the early 1990's to >3,000 in recent years; many of these are in the middle latitudes of the Southern Hemisphere. The Tropical Atmosphere/Ocean (TAO, McPhaden et al., 1998) array is a particularly noteworthy tethered array of buoys which took 10 years to construct (completed in 1994). With other buoys in the TRITON network after 2000, there became 70 moored buoys sampling the equatorial Pacific (at the surface and at depth). [Figure 2.5](#) illustrates the distribution of buoys at two different times in order to illustrate how the number of buoys has increased over time. Reflecting the growth in numbers, ERA-40 used about 1462 buoy observations per day during 1979-1990 and ~4000 per day during 1991-2001.

Finally, the Australian Bureau of Meteorology made estimates of sea level pressure based on manual analysis and interpretation of satellite imagery (Seaman and Hart, 2003). About 300 of these “PAOBs” were used each day in the ERA-40 reanalysis.

There are other observing systems but most are intended for special events (like dropsondes deployed within a hurricane) or for studying local boundary layer structures (like ground based profilers). Since those do not have global coverage they are not discussed further.

2.3 Sampling and spatial representativeness

2.3.1 Sampling

What are the implications of observing systems that sample the atmosphere in different ways? A radiosonde samples each level it passes through at one small spot. In contrast, a satellite sounding interrogates radiative energy emanating from a deep layer of the atmosphere over a horizontal area of hundreds (even thousands) of square kilometers. **Sampling** at short time interval at a small spot is more strongly influenced by short period and short length variations of the variable measured. Combining information from hours before and after the intended measurement time can introduce distortions for evolving flows. Sampling one type of geography with one observing system and another type with another system may introduce spurious differences in the climatology of the two types. Generally, when such differences become notable, they are noticed and resolved by the analysis procedure. Some of these implications are discussed in the remainder of this chapter.

2.3.2 Representativeness

What are the **implications of an uneven sampling** of the atmosphere? Some error estimates listed in **Table 2.1** have large ranges. In situ measurements of winds in the actual clouds used for CTW find quite small errors (1–3 m/s). Yet, when CTW are compared with nearby radiosonde stations, the apparent error is much larger (10–16 m/s). Similarly, commercial aircraft inertial navigation systems (INS) have small errors, but AIREP and ASDAR winds have much larger errors when compared to nearby radiosondes and nearby aircraft (Julian, 1983). These discrepancies arise because each system samples different time and space scales. Radiosondes ascend rapidly; aircraft traverse a large region in the horizontal quickly; CTW follow the ponderous motion of clouds that may be deep; each satellite sounding scans a large area; these are five very different paths to sampling the atmosphere! Therefore, the ranges in the **representativeness “error”** estimates are also measuring differences that arise due to variability of the atmosphere. The wide range of error estimates gives some indication of the representativeness of the data at a given grid point at a particular time. If the representativeness error is mainly due to **random errors, then time and zonal averages reduce** it.

The discussion of representativeness begs the question of what time and space scales must be resolved to **sample adequately** the atmosphere. Not surprisingly, the amount of resolution needed varies with the application. The World Meteorological Organization *minimum* requirements for a global, large scale observing network are listed in **Table 2.2**. Mohr (1984) and others propose stricter requirements than those listed in the table: perhaps twice as many vertical levels, perhaps half the horizontal spacing and somewhat higher instrument accuracy.

The **data coverage** varies with the location and the variable being considered. The surface-based observational network often provides dense observations over the midlatitude land masses at tropospheric and lower stratospheric levels. *Surface* observations from land stations, merchant ships, satellite scatterometers, and drifting buoys provide good global coverage of some variables (e.g. winds). *Tropopause level* winds and temperatures over the oceans and tropics can be deduced from satellites. The major remaining **gaps in the observational network** occur in the middle troposphere and above the tropopause over much of the ocean and some of the tropical land areas. These remaining gaps are being filled by satellite wind, moisture, and temperature profiles.

Grotjahn and Kennedy (1986, 1990) try to avoid the influence of a first guess on the estimate of the bias. They calculate comparison zonal averages of GCM data first using all model grid points, second using only those grid points near the stations shown in **Figure 2.1a**, and third using only grid points over major land areas. While not realistic, the second average reveals something about the sampling by radiosondes. The first two averages are remarkably similar, while the third set (major land areas only) is very different. The most important conclusion to draw here is that the radiosonde network, especially when supplemented by the other observing systems, is adequate to sample the larger scale general circulation features that will be discussed in this book.

Daley and Mayer (1986) use a GCM to study observational device errors and objective analysis errors in addition to the spatial bias. Daley and Mayer include simulated observations from the *non*-station network in addition to station-based data. The simulated observations also incorporate random and systematic errors for each device. Second, the simulated observations are interpolated using an operational objective analysis scheme. The simulated observations are taken from a 19.5 day (November period) run of a GCM.

The temperature errors over much of the troposphere are less than 2 K. The exceptions are at low levels in the high latitudes. Daley and Mayer feel that these errors partly reflect extrapolation problems in showing data below ground level (i.e., the South Pole is at high altitude, >2800m, and has surface pressure well below sea level pressure.) In the stratosphere the temperature errors are much larger and point to the unreliability of data, especially in the tropics. Geopotential height errors are shown to be generally less than 10 m except near Antarctica and in the tropical stratosphere. As expected from the hypsometric equation (C.13) since the temperatures are too warm, the heights are too high in the analysis both in the tropics and south of 70 S. Daley and Mayer do not find tropical, upper tropospheric westerlies in either their analysis or their GCM true state. Apparently, CTW are adequate to resolve this feature of the zonal average tropical zonal wind field.

The root mean square of the time and zonal average **transient error variance** is proportionally greater for the transient fields than for the time mean fields. Again the midlatitude errors are the smallest; transient temperature errors are typically about 20–25% of the true variance. The transient temperature fields have quite large errors in the tropics, in part because the temperature field has small true variance. The velocity field error over the Northern Hemisphere midlatitudes errors is 15–30% of the native variance; the error is about twice that in the Southern Hemisphere midlatitudes. The tropics have large fractional errors, again in part because the native variance is small. The error in the geopotential height variance increases with elevation. The ratio of error to native geopotential variance is 10–15% in most of the Northern Hemisphere middle latitudes, with slightly higher values in the Southern Hemisphere. In all the variance fields shown by Daley and Mayer, the errors are once again worst above Antarctica and in the stratosphere.

Atmospheric fields vary rapidly in time as well as in space. In some tropical locations the weekly and even the daily variation is comparable in magnitude to the seasonal cycle. How valid is it to calculate climatological, “general circulation” patterns from observations taken at one or two observing times per day? How valid is incorporating satellite soundings that are actually taken over a period lasting several hours before and after the observing time? The diurnal cycle creates an atmospheric tide with amplitude 1 hPa (at the surface) and wavenumber two shape, centered along the equator. Grotjahn and Kennedy (1986) find that the error in sampling the surface pressure field at just two times (simultaneously) looks like the tide. Assuming geostrophic balance holds as close as 5 degrees from the equator, then this pressure error pattern corresponds to meridional winds up to 2 m/s. However, the **time sampling error** was negligible for zonal averages. Oort (1978) found that gaps in the sequence of 12-hourly reports caused a smaller error than that from the unrepresentativeness of a radiosonde ascent and the spatial gaps between stations. Therefore, the diurnal cycle does not seem to alter significantly the results shown in this book. As for observations made outside a standard observing time, modern “four-dimensional” assimilation schemes allow data to be included at other times as part of the reanalysis procedure discussed next.

2.4 Data analysis

2.4.1 Data processing in analyses

As stated, most of the ‘observations’ shown in this book are reanalyses data. The **construction of these reanalyses** is briefly summarized.

After collection, observational data are processed in three ways: error checking, interpolation onto a regular grid, and initialization. Data analysis or more commonly data assimilation refers to these three steps. Extensive discussions are found in books by Daley (1991) and Kalnay (2003). The locations and accuracies of the observations are highly irregular. The data are more useful if projected onto a regularly-spaced grid in a systematic fashion. When this interpolation step is performed by a computer, it is called *objective analysis*. A common practice is to remove the gross errors during the objective analysis. For a variety of reasons, the objectively analyzed data at the grid points may not be consistent. When other fields are derived from the primary fields, small errors in the primary fields may swamp the signal being sought. The best illustration of this problem is the calculation of vertical velocity. Vertical velocity usually has large errors when calculated by the kinematic method from observed horizontal velocities. When calculated that way, vertical velocity comes from the small difference between two large quantities, a relationship that magnifies the errors in the horizontal wind measurements. Dynamical relationships can be incorporated into the objective analysis to balance the data in a process known as *initialization*. (Such balancing may be necessary because instrument and representativeness errors and processing steps change the values of variables in unnatural ways.)

Most objective analyses begin with a first guess at each grid point. The first guess is typically a model forecast (valid at the observing time). Schemes differ largely in the way nearby observations are weighted and combined to define the correction to the first guess. Schemes also differ in the skill of the model used. Usually several observations are present within a specified distance from the grid point. In areas where there are few observations, the correction may be unreliable because the consistency of a single observation cannot be checked against other observations. Areas with few observations typically rely more heavily upon less accurate observing devices. For example, operational centers place a heavy reliance upon satellite data over the southern oceans because there are few alternatives. One consequence is the rejection of radiosonde data at isolated land stations because those data differ too greatly from the first guess, where the first guess came from a forecast that was largely influenced only by satellite observations upstream. Trenberth and Olson (1988) suggest that some operational analysis schemes place too much emphasis on the first guess in the Southern Hemisphere. Nonetheless, having satellite observations is far better than nothing.

In general, the *data assimilation* adapts to the irregular sampling times in some fashion, either by binning observations from an assimilation period (6 hours, say) to apply to one observing time. Modern schemes used at weather forecast centers introduce the observations as the integration of the forecast model proceeds in time.

2.3.2 *Different data assimilation, different circulations*

Data assimilation is needed to produce the gridded reanalysis datasets emphasized in this book: NDRA2 and ERA-40. These schemes are not as elaborate as those used by operational weather forecast centers because of the long periods of data (and much lower model resolution) being analyzed. The schemes used for reanalysis are similar to operational ones. Parrish and Derber (1992) and Kalnay et al. (1996) describe the assimilation system used for NDRA2. ERA-40 used an assimilation system patterned after that described in Andersson et al. (1998). These schemes require a weather forecast model to produce an estimate of the values of a variable on a regular grid, known as the “first guess” for that variable. For example, the ERA-40 first guess is a 9 hour forecast produced from a prior analysis that in turn was produced from observations that modified a first guess, etc.

The model used in the NDRA2 has 28 levels and uses triangular horizontal truncation that includes up to 62 (zonal) wavenumbers (“T62”). T62 corresponds to a 192 (longitude) by 94 (latitude) Gaussian grid. It is based on the model described in Kanamitsu (1989). The ERA-40 model uses 60 levels and T159 horizontal spectral resolution interpolated to a Gaussian grid with ~125 km spacing (approximately 320 by 160, declining towards each pole). Much of the NDRA2 and ERA-40 data shown here have been ‘upscaled’ to a lower-resolution 2.5 by 2.5 degree (144 longitude points by 73 latitude points) grid. Both reanalyses produce data at 0, 6, 12, and 18 GMT each day. The NDRA2 dataset starts with 1979, and has continued in near real time. The ERA-40 dataset is a 45 year period from September 1957 through August 2002. The ERA-40 data record was succeeded by an ongoing reanalysis labeled “ERA-Interim” that begins in 1979. ERA-Interim uses a more advanced assimilation system and finer horizontal resolution (Berrisford et al., 2011) at 6 hour intervals. Other reanalysis datasets exist at the time of this writing.

When reanalyses are used to display individual variables, differences between the analyses occasionally occur. Some of the difference is due to the forecast model differences (e.g. model resolution, topographic elevations used, boundary properties like snow cover, etc.). Additional differences are expected due to the different input data. The differences in input data used by NDRA2 and ERA-40 are summarized in [Table 2.3](#), reproduced from Grotjahn (2008). Differences in the assimilation procedures of NDRA2 and ERA-40 are summarized in [Table 2.4](#).

2.5 Compositing

The global coverage of observing systems has large gaps. In addition, the atmosphere contains many diverse and variable phenomena. These two facts frequently lead researchers to

composite their observations, because compositing improves their ability to draw meaningful conclusions about atmospheric behavior. Zonal averaging and especially time averaging are two common examples of compositing. **Table 2.2** shows that the atmosphere can be very well sampled with observations that are rather widely spaced (500 to 1000 km apart). While individual storms move rapidly and vary in intensity and many other properties, their simple statistical properties (like mean and variance) tend to be stable over some period of time. Therefore, time averaging, especially when done separately for different seasons, can usefully depict the general properties discussed in this book.

Appendix A defines the symbols used throughout the book to indicate specific types of averaging as well as how different averages can be applied in combination to isolate specific features of the general circulation.

The first question to ask when **compositing is: what length of time (or space)** average is needed? For the persistent part of the general circulation, one anticipates that a month is a minimal time interval over which to average. Longer time periods, especially periods longer than several years are even better. Each winter, for example, would be an independent sample. Longer time averages reduce the effect of individual, atypical weather periods; the data and conclusions are not dominated by an unusually severe winter event, for example. To separate seasonal variation, Blackmon et al. (1977) average data from each January from a 30 year period. But time averages throw out some important details. One would not expect time average fields to satisfy all the dynamical constraints. **Averaging smears out many small-scale properties** that typically meander or change with time. For example, the time and zonal average subtropical jet stream is much less unstable to the formation of frontal cyclones than local regions of the jet on specific days. The reason is that the jet has larger vertical and horizontal shears in the latter case. Hence, the time and zonal mean flow might not predict the formation (or at the least, the strength) of the ubiquitous frontal systems. Another problem is that the neglected features may be necessary to maintain the average field. A prime example is the zonal average wind fields; they cannot be explained except when the momentum fluxes by zonally-varying eddies are included.

Generally speaking, the length of time needed to obtain a representative time average depends upon the area in question. When the average is over the whole hemisphere, then the averaging period can be rather short. James (1983) finds 15–30 days are adequate for the meridional heat flux, but *only when averaged over the whole hemisphere*. By implication, 15 days is a reasonable minimum time sample for most other variables. When the averaging domain becomes smaller (e.g., a zonal average only), then the averaging period needed usually must be longer. There appears to be no consensus regarding how **much time is adequate for time averages**

and for combined zonal with time averages. Sometimes the averaging period is dictated by the length of accurate data available.

The eddy momentum flux is one major field that is notoriously difficult to measure. The eddy momentum flux is not statistically stable on 30-day averages according to Blackmon et al. (1977). A much longer period average is recommended for this quantity.

This book presents observations by first discussing zonal and then time average distributions. **Why zonal average?** Zonal averaging is useful when a planet's circulation has small eddies compared to zonal mean flows. In a dynamical viewpoint, Williams (1978, 1979) relates the predominance of zonal jets versus more turbulent flow patterns to the Rhines (1975) **transitional wavenumber**: $k_{\beta} = (\beta/2U_s)^{1/2}$. For a rapidly rotating planet, k_{β} is large and the turbulent eddies have small length scale, such as the turbulent eddies superimposed on multiple jets for the banded circulation of Jupiter. For the Earth (Williams, 1979) the situation is less clear because other factors (notably topography and surface drag) disrupt the zonality. Other properties that change with rotation are summarized in James (1994). While other factors are important in determining the circulation of a planetary atmosphere, rotation rate is convenient to make a point that the appropriate averaging to choose depends upon the symmetries characterizing a circulation. A simple thermodynamic argument can support the use of zonal averages as well. Earth rotates swiftly enough so that the distribution of solar input is rather evenly spread around a latitude belt before a significant amount of heat can be transported away to the cooler regions. As discussed in §1.2.1, the **radiative cooling rates** are slow enough so that large temperature differences are not set up between night and day sides of the planet. So, zonal averages can tell us useful things about the atmosphere's circulations and thermal patterns. However, the zonally-varying features must also be considered because Earth's atmosphere interacts strongly with the surface. **Figure 2.6** shows important features that are *not* zonally symmetric. For example, comma-shaped cloud bands associated with vigorous frontal cyclones march across the southern ocean. While cloud patterns over the tropical oceans are somewhat zonally symmetric notable zonal asymmetries are visible. Even the equatorial **intertropical convergence zone** (ICZ) is composed of numerous small clouds (mainly individual thunderstorms) whose number and density vary along the ICZ. Important zonal variations in Earth's atmosphere result from longitudinal variations of topography, land and sea area, vegetation type and snow cover, and from the **hydrodynamic instability** of the currents set up by the latitude-varying distribution of incoming solar radiation. For example, in the subtropical oceans west of South America (low) clouds blanket the ocean while much of the adjacent continent has few clouds. Later chapters will discuss most of these zonal variations and their sources.

Problems

1. *Observation counts.* Estimate the number of observations taken each day using information in Table 2.1. Assume the following.

- (i) One “observation” equals one scalar variable at one level at one time.
- (ii) Vector horizontal winds are 2 scalar variables. Each satellite wind is at only 1 level.
- (iii) Where ranges are given in the table, use the larger value.
- (iv) A “report” in the table can include many “observations” as defined here.
- (v) That only 10 “standard” levels are obtained from each radiosonde/rawinsonde sounding.

Assume each satellite temperature sounding is 20 values.

Show your estimates for each of the observing systems listed in the table separately, then indicate the “grand total”.

2. *Rough economics of observing systems.* Very roughly estimate the relative costs of sampling the atmosphere by radiosondes versus by satellites 4 times daily for 5 years. Assume that each geostationary weather satellite: costs 300 M Euros to build and put into orbit, takes 4000 soundings each day, and lasts for 5 years. Assume 5 satellites can cover most of the globe (high latitudes excluded).

Assume that radiosondes could be dropped from 9,500 drones flying at high altitude over the oceans and from 1000 land stations. Assume that each radiosonde costs 20 Euros and each station and drone releases two radiosondes 4 times each day. Assume that each drone costs 100,000 Euros to build and 300 Euros each day to maintain.

Assume that the costs of receiving the data are the same and neglect that cost for this calculation. Ignore the difference in vertical resolution of winds and moisture for the three systems.

- a. Estimate the total cost for 5 years of each system.
- b. Estimate the cost per observation for each system, assuming each sounding produces 20 observations. (temperature and wind only)

3. *Orbital periods and elevation.* A satellite orbiting the Earth in a circular orbit follows a balance between centrifugal acceleration outward (a_{sat}) and the gravitational acceleration inward g_{sat} . Where $a_{\text{sat}} = \Omega_{\text{sat}} r_{\text{sat}}^2$ while Ω_{sat} is the angular velocity (rad/s) of the satellite and r_{sat} is the distance of the satellite from the center of the Earth. Similarly, $g_{\text{sat}} = G M_{\text{Earth}} / (r_{\text{sat}})^2$ where G is the gravitational constant ($= 6.67 \times 10^{-11} \text{ m}^2 \text{ s}^{-2} \text{ kg}^{-1}$) and M is the mass of the Earth ($= 6 \times 10^{24} \text{ kg}$).

- a. Find the distance above the Earth for a geostationary orbit. (period equals 24 hr)
- b. Find the distance above the Earth for a polar orbiting satellite. (period equals 100 minutes)
- c. A space station orbits the Earth on average at 400km. How long (in minutes) does it take to orbit the Earth once? How many orbits does it complete in one 24 hr day?

4. *Arcing path from latitudinal motion.* In Chapter 1, an imaginary circulation which we labelled as a Hadley cell was drawn whereby the upper level circulation included westerly as well as poleward components. This problem identifies what orientation to draw those circulations. It might also describe motion of an air parcel or even a balloon if one makes the major assumption of no slowing by friction.

Consider a parcel that moves from 10 N to 30 N with a constant meridional component of velocity that equals 2 m/s. Assume that friction is negligible. The parcel is initially at longitude 0 degrees and has $u=U_0$ zonal velocity.

- a. Write down expressions relating meridional (y) and zonal (x) distance to longitude (λ) and latitude (ϕ), respectively. From those formulate definitions of v (northward) and u (eastward) velocity using λ and ϕ .
- b. Derive the general formula for radians of longitude travelled when proceeding from latitude ϕ_S to latitude ϕ_N . The formula should not contain any unsolved integrals. *Hint: use part a. to convert between radians and distance and between time and space.*
- c. Use your formula to find the ending longitude when the parcel reaches $\phi_N = 30$ N. Let the initial conditions be $u=0$ at 0 degrees longitude and $\phi_S = 10$ N.

5. *Eddy momentum flux convergences.* Assume that a streamfunction field Ψ is defined:

$$\Psi = \sin(x + A y) \cos(y) - \sin(B y)$$

Where $\pi/2 \leq x \leq 2\pi + \pi/2$ and $-\pi/2 \leq y \leq \pi/2$. Also, A and B are constants. Note that $u = -\partial\Psi/\partial y$ and $v = \partial\Psi/\partial x$. To add additional interest, leave A and B as a variable in your solution and in your plotting program. Use one value each of A and B below:

Let $A = -0.9, -1.5, -0.5, -0.5, 0.5, 1.0, -0.3$ and $B = 1.2, 1.5, 1.5, 1., 1., 1.5, 1.5$

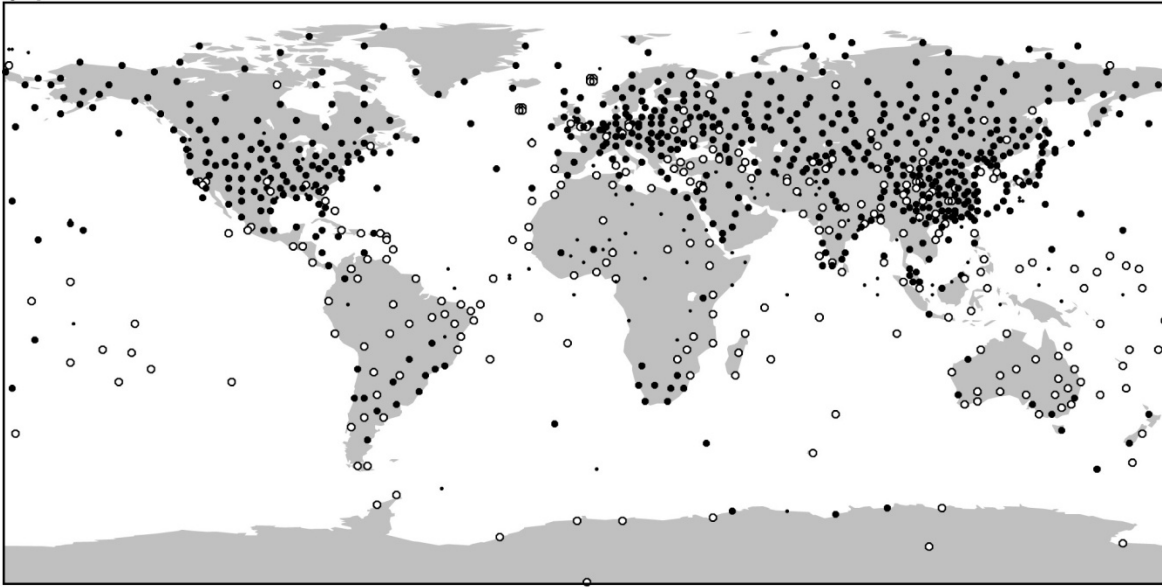
- a. Derive the general form of the zonal average of the eddy momentum flux: $[uv]$. Solve all integrals (it simplifies greatly). *Hint: your result should only be a function of A and y .*
- b. Derive the formula for zonal mean eddy momentum convergence, $-d[uv]/dy$.

c. Make contour plots of Ψ and uv for the A and B specified over the x and y ranges given. Use at least 21 grid points in y and 41 grid points in x . Clearly label axes and contour lines.

d. Make a single plot containing: $[\Psi]$, $[u]$, $[uv]$, and $-d[uv]/dy$ for the A and B chosen over the y range given. Use 21 grid points in y . Clearly label axes and contour lines.

e. How does the shape of the Ψ field vary for negative, zero, and positive values of A ? How does that change of shape relate to the sign of the value $[uv]$ at $y=0$?

(a) 1979



(b) 2001

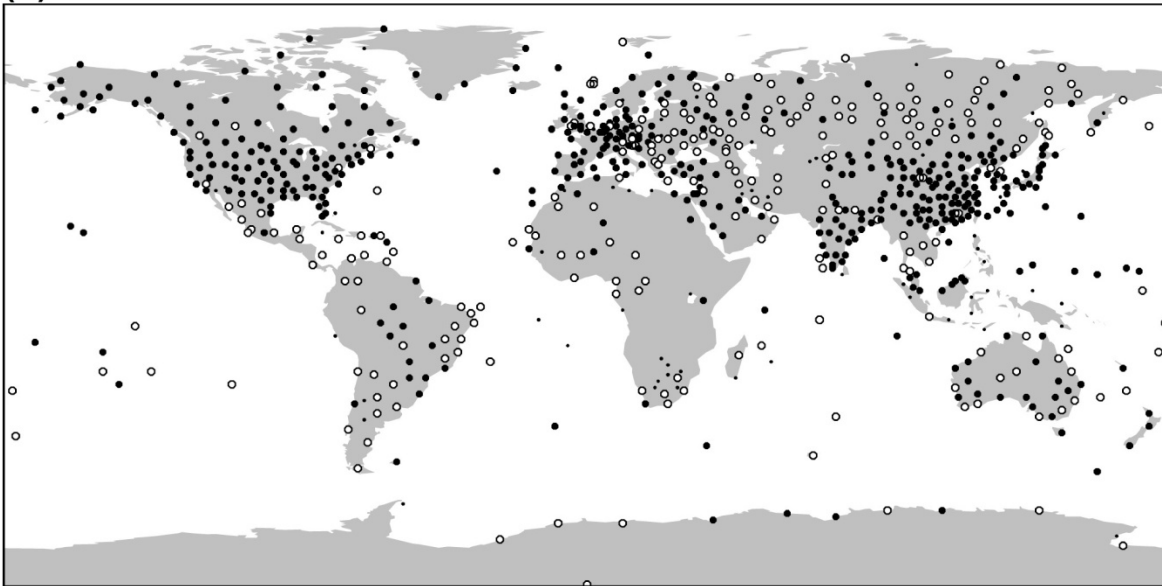


Figure. 2.1 Radiosonde station locations and frequency of report as used by the ERA-40 dataset during two indicated years (a) 1979 and (b) 2001. Stations reporting at least three times every 2 days are identified with larger dark circles. Open circles are used when reports are at least once but less than three times every 2 days. Stations reporting less than once per day but at least once per week are marked with a small dot. Figure reproduced with permission from Uppala et al., 2005.

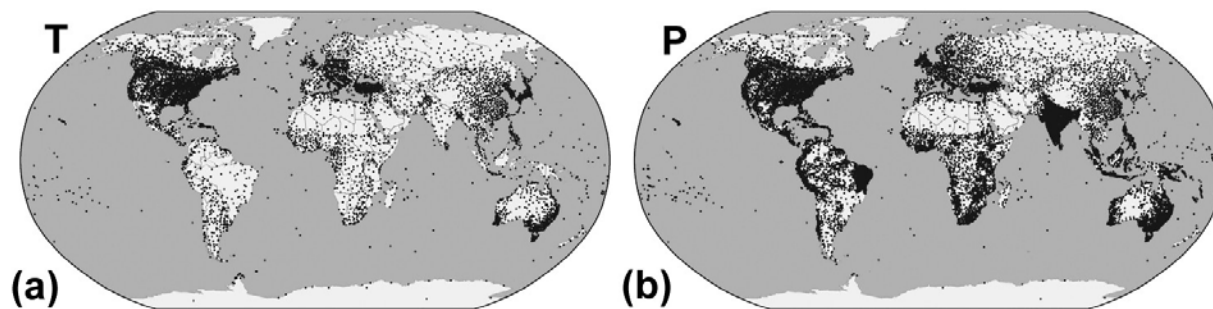


Figure. 2.2 Surface weather data stations in the global historical climatology network reporting monthly mean values of (a) temperature (7,280 stations) and (b) precipitation (20,590 stations). Figures provided by the National Climatic Data Center of the U.S. National Oceanographic and Atmospheric Administration.

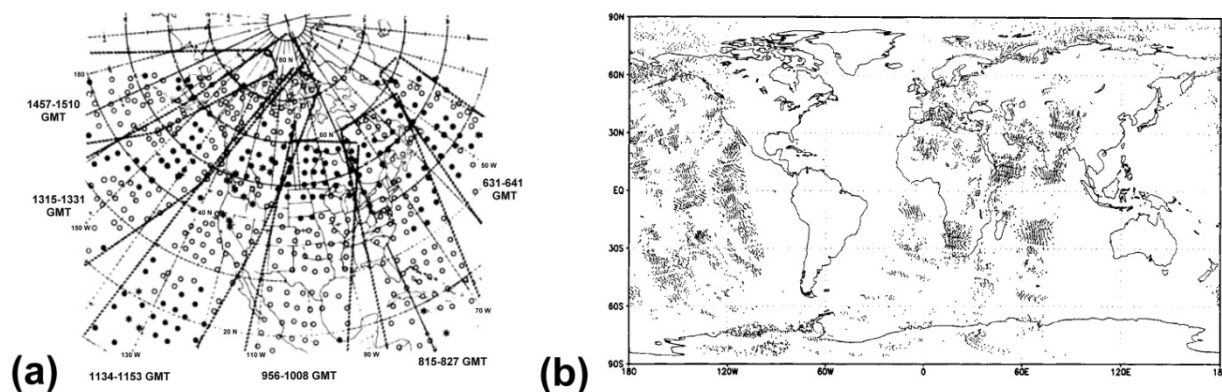
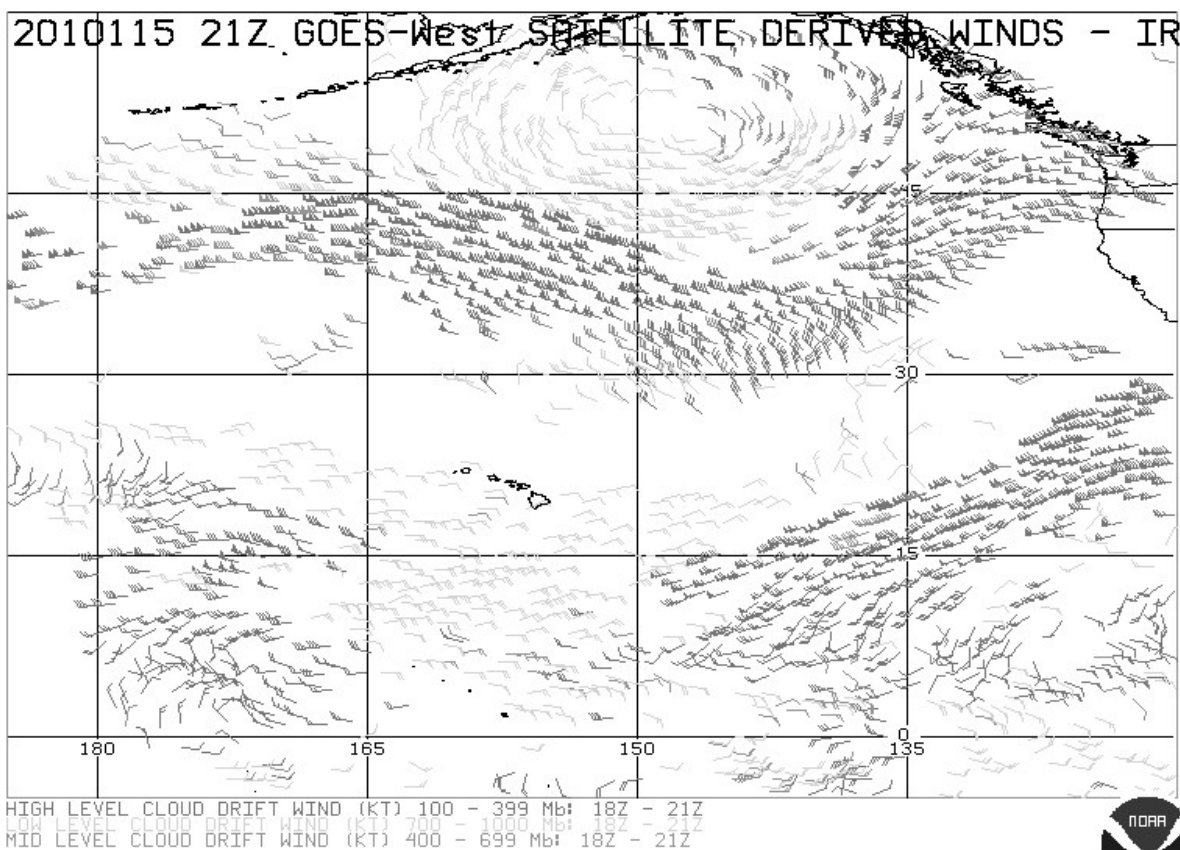


Figure. 2.3 (a) Illustrative example of swath paths (dashed lines) scanned by each orbital pass of the TIROS-N satellite. Time periods of the passage overhead are indicated using Greenwich Mean Time (GMT); the swaths occur at a similar time of day locally. Circles mark locations of temperature retrievals from the satellite on 6 April 1979. Shaded circles distinguish retrievals through cloudy sky, asterisks for partly cloud paths, and open circles for clear sky paths. Figure from Smith (1985). (b) Sounding locations (dots) of the NOAA-12 and NOAA-14 satellites HIRS data on 22 March 1997 as might be included in ERA-40 data. Reproduced from McNally et al. (2000). One can clearly see improved resolution with more recent satellite data.



1 2010115 (25 APR 10) 21Z GOES-WEST HIGH DENSITY SATELLITE WINDS - IR - NW SECTOR LDRS

Figure. 2.4 Example of satellite derived cloud drift winds from the GOES west platform on 25 April 2010. Individual winds are indicated with wind barbs and are grouped to three levels. Lower level winds from 1000-700 hPa are lighted shaded, medium shading is used for winds assigned to 699-400 hPa, and darker shading is used for higher winds (399-100 hPa). Figure reproduced from the NOAA Satellite Information Service.

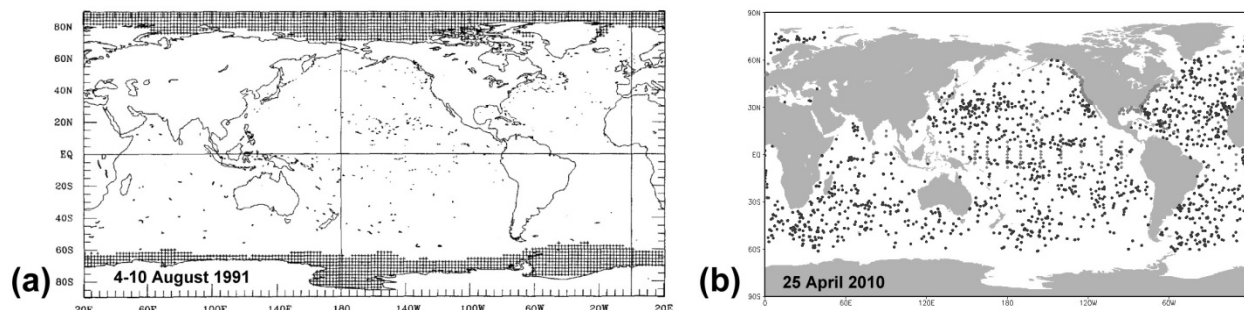


Figure. 2.5 Examples illustrating the growth of the numbers of drifting and moored buoys.(a) buoys during the week of 4-10 August 1991 (approximately 200 buoys). Reproduced from Reynolds and Smith (1994). (b) Buoys on 25 April 2010 (2359 buoys). Darker dots are drifting buoys, lighter dots are moored buoys.



Figure. 2.6 Composite image of the Earth from space on 27 January 2007. Image created by R. Stöckli at the NASA GSFC.

Table 2.1 Properties of various operational observing systems.

Observing system	Fields observed	Error		Time resolution	Coverage	Vertical resolution	Horizontal resolution	Comments and (reports/day)
		Random error	Remarks					
Surface land stations	P_S T_S V_S rh_S	± 0.5 mb $\pm 1^\circ\text{C}$ $\pm 1.5 - 3$ m/s $\pm 10\%$	–	≥ 3 hours	WWW-network (fixed locations).	–	≥ 50 km	high resolution over most land areas. 4,095 of 9,500 stations in WWW (20,000/day; in 1992) (27,500 metar/day; in 2000)

Rawinsonde & radiosonde Soundings	T	$\pm 0.5-2.^\circ\text{C}$	$> \pm 2^\circ\text{C}$ in Stratosphere. below 500 mb. above 500 mb.	6–12 hours	WWW- network (fixed locations)	~50 mb	≥ 300 km (see Figure 2.1)	About 885 stations (1200 soundings/day). 5 ocean weather ships by 1990. By 2000, no more ships, ~670 stations. About 600 pibal stations (1000 soundings/day): wind only in 1990. By 2000, 74 stations
	rh	$\pm 5\%$	Much larger for $T < -40^\circ\text{C}$					
Buoys, Ocean platforms (incl. oil rigs, etc.)	P_S	± 1 mb	very few	6–12 hours	Originally mainly used south of 20°S and N.		500–1000 km	130–200 were operational during GWE. 300 (2500/da) plus ~170 (600/da) are moored in 1990. Only
	T_S	$\pm 1^\circ\text{C}?$	measure V_S or air temperature					
	V_S	$\pm ?$						

					Atlantic.			moored measure V_s . By
					Later			2000: ~2,200 drifting
					coverage is			and 915 moored.
					global			
Merchant	P_s	± 0.5 mb	assumed	≥ 3 hours	main		varies	About 7,400 ships
Ships:	T_s	$\pm 1^\circ\text{C}$	same as for		shipping		greatly	(3500/da) in 1990. By
(1) Surface	V_s	$\pm 1.5\text{--}3$ m/s	surface land		routes			2000: 777 ships. Few
Only	rh_s	$\pm 10\%$	station					ships in southern oceans
(2) ASAP or	T	$\pm 1^\circ\text{C}$	assumed	≥ 12 hours	main	~ 50 mb	varies	About 15 ships (30/da)
other upper air	V	± 3 m/s	same as for		shipping		greatly	equipped by 1989
	rh	$\pm 10\%$	radiosondes		routes			
Commercial								
Aircraft:								
(1) Post-flight	V	± 6 m/s	less error for	continuous	commercial	200–300	500–1000	(~100 reports per day)
reports			inertial		1 air routes	mb level	km	roughly 10 observations
			navigation			only		per report

system (INS)

(2) AMDAR	T	$\pm 0.5-1^{\circ}\text{C}$	possible ± 10	continuous	200–300	110 km		ASDAR on about 40
	V	$\pm 0.5-3$ m/s	m/s error in representative ness. Double values when comparing to radiosondes	commercial air routes	mb level (see comments)	along flight path		aircraft (est for 1986). 4000 craft in 2009; (~140,000 obs./day). Also takes “soundings” when plane takes off and lands. Few obs (150/day) in 1990
(3) AIREP	T	$\pm 1^{\circ}\text{C}?$	location	continuous	commercial	200–300	concentrat	About 3,000 aircraft
	V	$\pm 0.5-3$ m/s	errors. ± 10 m/s representative ness		l air routes	mb level	e along every tenth meridian d	(4,500/day) By 2000: ~1,100 AIREPS/day

Satellite:

(1) Vertical	T	$\pm 1.5-3.5^{\circ}\text{C}$	larger errors	continuous	global	~200 mb	40 km	(About 6,000
--------------	---	-------------------------------	---------------	------------	--------	---------	-------	--------------

Temperature soundings	$\pm 2^\circ \text{C}$ is typical	in clouds. Estimates shown are for a single level; T values over a layer are better			(3-5km in troposphere)	possible, typically ~500 km	soundings/day) in 1990. By 2000: (20,400 GOES plus 15,000 Polar soundings per day). (258,000 radiances/day)
(2) GPS/MET (LIMS)	T, e	$\pm 0.5-2^\circ \text{C}$? Or, a few mb	Depends on accuracy of other variable	continuous global	~1km or less in much smaller steps	~500 per day over the globe.	Need an independent measurement of T other to get e or <i>vice versa</i> . Might neglect moisture in stratosphere where e is very small.
(3) Vertical water vapor sounder	TCPW Or WV or rh in	2-4 kg/m ² error std ?	large errors in clouds	continuous global	~400 mb	~50 km	

	layers	±20– 30%						
(4) Cloud-track winds (CTW)	V	±4.5–5.5 m/s for low level CTW ±9–10 m/s for high level CTW	In situ measurement s of winds suggest much smaller error of 1–3 m/s	continuous	55° N to 55°S	200–500 mb	See Fig. 2.6 30–400 km	(About 6,000/day in 1983). (7,000/day in 1990) (>45,000 per day by 2000) Most are over oceans. Speed bias 0.5–1.6 m/s. Newer systems 1–7 m/s better than old.
(5) Scatterometer	V _s	±0.5–2 m/s <17 degrees	Rms errors	continuous	25-50 km over ~600 km swath	Ocean surface		(~58,000 values/day)

Data in this table were based on information in various sources, such as: Freilich and Dunbar (1999), Halem et al. (1981, 1982), Hasler et al. (1979), Hurrell et al. (2000), Luers and Eskridge (1995), Liu et al. (1992), NOAA websites (CPC, ESRL, NCEP, NDBC, NESDIS, OSDPD, PMEL, SSD), Soden and Bretherton (1994), Spencer and Christy (1992), UCAR MetEd website, Ware et al. (1996), WMO (1991, 1996).

Table 2.2 Observational requirements for a global observing network from the WMO (1990) and Mohr (1984).

	Horizontal Resolution	Vertical Resolution	Accuracy (RMS)	Frequency of Observation
Temperature	500 km (1000 km over tropical oceans)	4 tropospheric levels 3 in stratosphere	$\pm 1^\circ\text{C}$	every 12 hrs
Wind	500 km	4 tropospheric levels 3 in stratosphere	± 3 m/s	every 12 hrs
Relative Humidity	500 km	4 layers or 2 parameter vertical function	$\pm 30\%$	every 12 hrs
Sea-surface Temperature	500 km	–	$\pm 1^\circ\text{C}$	perhaps 3-day averages of instantaneous measurements
Surface Pressure	500 km	–	$\pm 0.3\%$	every 12 hrs
Precipitation	100 km	3km	50%	every 6 hrs

Table 2.3 Some aspects of the NDRa2 and ERA-40 input data Note: not all data were available during the full length of the assimilated period. See the original references for details. Acronyms and abbreviations are defined in the appendix. From Grotjahn (2008)		
Dataset	NDRa2	ERA-40
Primary reference	Kanamitsu et al. (2002)	Uppala et al. (2005)
Input Data		
Satellite data:	NESDIS TOVS temperature retrievals, Cloud track winds. (No moisture data used)	Direct assimilation of VTPR, TOVS (HIRS, MSU, SSU) and AMSU-A Level-1c radiances, Atmospheric Motion Vectors, scatterometer winds, SSM/I radiances as 1D-Var retrievals of TCWV and surface wind speed TOMS and SBUV data in ozone analysis, Altimeter wave height data (see Hernandez et al., 2004)
Upper air data	Radiosondes, dropsondes, pibals, aircraft data, wind profilers	Radiosondes, dropsondes, pibals, aircraft data, wind profilers
Surface data (snow cover)	Stations, ships, buoys, PAOBs, (NSIDC-based, USAF snow cover after fall 1998, depth is dynamic)	Stations, ships, buoys, PAOBs. (SYNOP snow depth, most after 1976)
SST and Sea Ice	AMIP-II (should be same as ERA-40 except for time interpolation, Kanamitsu, pers. comm., 2007), Reynolds SST after 1999	Reynolds et al. (2002), Rayner et al. (2003) and other NCEP products
Period	1979- present	September 1957-August 2002 (45 years)

Table 2.4 Some aspects of the NDRa2 and ERA-40 assimilation systems. Acronyms and abbreviations are defined in the appendix. From Grotjahn (2008)		
Dataset	NDRa2	ERA-40
Primary reference	Kanamitsu et al. (2002)	Uppala et al. (2005)
Period	1979- present	September 1957-August 2002 (45 years)
Assimilation model		
Model based on:	MRF (ca 1995, with modifications) full radiation calculation hourly	ECMWF forecast model CY23r4 (operational in June 2001)
Assimilation scheme	3DVAR (Parrish and Derber, 1992)	3DVAR-FGAT, OI for surface parameters and ocean wave height
Horizontal type, resolution (grid type, in latitude x longitude)	Spectral, T62 (Gaussian, 94 x 192 for dynamics and physics)	Spectral, T159 (linear reduced Gaussian grid 160 by up to 320, declining for latitudes >27°), (Hortal and Simmons, 1991)
Vertical coordinate type, number of levels	Sigma, 28	Hybrid sigma (Simmons and Burridge, 1981), 60
Horizontal grid, levels used here	2.5° latitude by 2.5° longitude, 17 levels	2.5° latitude by 2.5° longitude, 17 levels
Parameterizations		
Orography	Smoothed mean orography to remove Gibbs oscillations.	Smoothed mean orography
Land surface	Pan and Mahrt (1987), Mahrt and Pan (1984) Soil moisture correction based on model minus observed precipitation	Viterbo and Beljaars (1995) Van den Hurk et al (2000)
PBL	Hong and Pan (1996)	Beljaars and Viterbo (1998), Viterbo et al. (1999)
Radiation	Chou (1992), Chou and Lee (1996) (shortwave) Fels and Schwarzkopf (1975) (longwave)	Morcrette et al (2002a), (shortwave), Morcrette et al (2002b), (longwave) See also Gregory et al. (2000)
Time varying radiatively active: gases / aerosols (i.e. volcanic eruptions)	No (CO ₂ constant) / No	Yes (CO ₂ , CH ₄ , N ₂ O, CFC-11, CFC-12, based on Houghton, et al., 1996) / No
Convection	Simplified Arakawa Schubert, Grell (1993)	Tiedtke (1989) type, see Gregory et al. (2000)